Physically Derived Synthesis Model of an Edge Tone

Rod Selfridge[1], Joshua D Reiss[2], and Eldad J Avital[3]

[1]*Media and Arts Technology Doctoral College, SEECS,* [2]*Centre for Digital Music, SEECS,* [3]*Centre for Simulation and Applied Mechanics, SEMS,* [1,2,3]*Queen Mary University of London, Mile End Road, London, UK.*

Correspondence should be addressed to Rod Selfridge (`r.selfridge@qmul.ac.uk`)

ABSTRACT

The edge tone is the sound generated when a planar jet of air from a nozzle comes into contact with a wedge and a number of physical conditions are met. Fluid dynamics equations were used to synthesise authentic edge tones without the need for complex computation. A real-time physically derived synthesis model was designed using the jet airspeed and nozzle exit-to-wedge geometry. We compare different theoretical equations used to predict the tone frequency. A decision tree derived from machine learning based on previously published experimental results was used to predict the correct mode of operation. Results showed an accurate implementation for mode selection, and highlighted areas where operation follows or deviates from previously published data.

1 Introduction

Aeroacoustic sounds are the class of sounds generated by air flowing in a wake or interacting with boundaries. The sounds can also be generated by objects moving through the air. Examples of aeroacoustic sounds are those created by a sword swinging through the air [1] or a spinning propeller [2]. Aeroacoustics can also couple with mechanical vibrations to produce sound as in the Aeolian harp [3].

It was shown in [4] that aeroacoustic sounds in low flow speed situations could be modelled by the summation of compact sound sources, namely monopoles, dipoles and quadrupoles. An acoustic monopole, under ideal conditions, can be described as a pulsating sphere, much smaller than the acoustic wavelength. A dipole, under ideal conditions, is equivalent to two monopoles separated by a small distance but of opposite phase. Quadrupoles are two dipoles separated by a small distance with opposite phases. A longitudinal quadrupole has the dipoles axes in the same line while a lateral

quadrupole can be considered as four monopoles at the corners of a rectangle [5].

The edge tone is the sound generated when a planar jet of air from a nozzle comes into contact with a wedge or edge and a number of physical conditions are met. Research was undertaken to accurately determine the frequencies, gain and propagation patterns required to replicate the edge tone. Key semi-empirical formulas were found within aeroacoustic research, allowing us to identify relationships and parameters. Semi-empirical equations are those where an assumption or generalisation has been made to simplify the calculation or yield results in accordance with observations.

Physical models for sound synthesis are those which model the underlying physics which produce a sound. They allow users to change parameters and be confident that the underlying laws and principles are consistently obeyed, giving the produced sounds an inherent authenticity. The development of real-time sound synthesis

models has great potential for use in nonlinear media such as virtual reality and games.

The edge tone is one of the fundamental aeroacoustic sounds. Two examples of real-time physically derived synthesis models of aeroacoustic sounds were given in [6] for Aeolian tones and in [7] for cavity tones. Examples of how these models can be used for real-time sound effects was shown in [8].

The most common use of edge tones is as an excitation source for flue instruments such as a flute, recorder or pipe organ. In these instruments, the edge tone is coupled to a tube, exciting the tube's resonant frequencies. Varying the tube length produces the desired musical pitch.

A flute sound was synthesised in [9] where a digital waveguide was used to capture the most relevant physical characteristics while signal-based analysis / synthesis techniques was used to capture perceptual effects. In this model, the excitation signal was obtained by deconvolution of resonator transfer function with a real flute sound.

Real-time synthesis of a physical model of a flute was presented in [10] where the excitation source and resonator of the tube body were split into lumped models. Although we focus purely on the edge tone, it is believed the approach undertaken for flue instruments in [10] is similar to ours.

The edge tone was described as a special type of impinging tone [11] where self-sustained oscillations are generated as a jet impinges on a flat plate rather than a wedge. Impinging tones are known to occur between the ground and the jet created by vertical take-off and landing (VTOL) aircraft, in transonic wind tunnels, and from pressure and velocity probes.

Compact sound source models of an edge tone derived from physics allows modelling of edge tones that appear in recorders, flutes and other flue musical instruments. The fluid dynamics process involves a feedback system similar to other tones such as the cavity tone, plate tone and hole tone. They could also provide real-time sound effects when synthesising the sound of a VTOL aircraft near the ground, a boiling kettle or a police whistle.
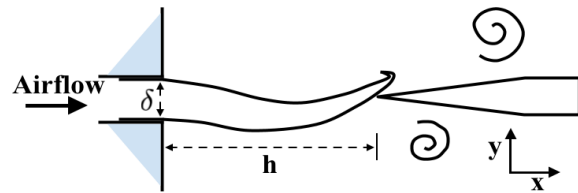

Fig. 1: Diagram of an edge tone flow showing nozzle exit width δ and nozzle to edge width h

2 Fluid Dynamic Principles

Figure 1 shows the basic geometry under which the edge tone is generated and studied. A jet of air is inherently unstable and as the jet travels between the nozzle exit and wedge these instabilities are amplified. At the wedge, the air stream sheds vortices on alternate sides and an oscillating pressure force is generated. The pressure pulses travel back towards the nozzle exit and at certain frequencies, disturb the unstable jet creating a self-sustained feedback system. The oscillating pressure generates sound which is modelled as a dipole compact sound source located near the wedge tip.

The distance between the nozzle exit and the wedge h can be varied, as can the exit width δ. Some studies also vary the position of the wedge with respect to the centre of the jet, (y axis). This is common in flue instruments but beyond the scope of this paper which will assume the wedge is positioned at the centre of the jet, $\delta/2$. The jet airspeed u is a further important parameter. Readers are directed to [12] for a review of theoretical and experimental studies.

Different types of jet profiles are described in the literature; *Parabolic* or *Top Hat* are the most common. These depend on the length of the channel prior to the nozzle exit, known as the flue.

A parabolic profile is created from a flue channel where the length is such that the airspeed at the walls reduced. This is due to a significant growth of the boundary layers on the flue wall and results in a parabolic profile at the nozzle exit. A top hat jet profile is created from a short flue length. Here the boundary layers developing on the flue walls have not grown much and thus give a top hat type shape, (more rectangular), at the nozzle exit.

The fluid dynamics of the edge tone ([12] and references therein) have been studied, but the complex behaviour is not yet fully understood. One observation is that the edge tone frequency varies with u and h.
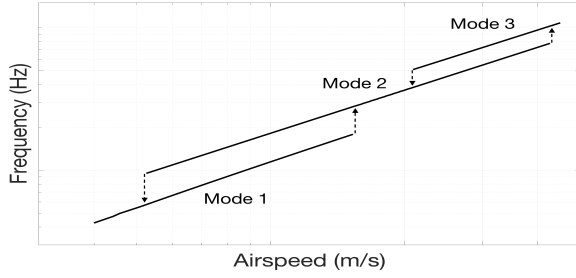
Fig. 2: Example of ideal mode changes, including hysteresis, as airspeed u varies with fixed h
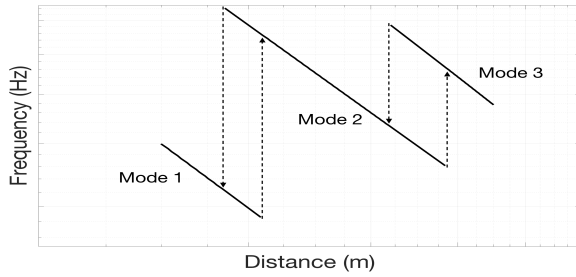

Fig. 3: Example of ideal mode changes, including hysteresis, as distance h varies with fixed h

A number of frequency stages or modes exist when these parameters are varied, with hysteresis observed between the mode changes. An ideal plot of the changes in the frequencies as u is varied is given in Fig. 2, an ideal plot for mode frequency change due to varying h is shown in Fig. 3.

2.1 Frequency Predictions

Studies have defined semi-empirical equations to predict frequencies f_k, where k is the mode number. The first notable experimental study was carried out by Brown [13] who stated the formula given in Eqn. 1 to calculate the edge tone frequency:

$$f_k = C_k(100u - 40)(\frac{1}{100h} - 0.07)0.466 \quad (1)$$

where the coefficients for C_k are 1, 2.3, 3.8 and 5.4 for mode numbers $k = 1$, 2, 3 and 4 respectively. Brown [13] found that the limits for the ratio of the distance h and nozzle exit width δ are 3.5–60. He also noted that the first frequency mode coexisted with other modes but at a decrease of about 7%.

The edge tone phenomenon caused by vortices travelling in the air jet as generated by periodic disturbances at the nozzle exit was modelled in Holger et. al. [14].

Through analysis of the interaction between the vortices and the edge, the oscillating flow at the exit can be estimated. This enables an estimate of the phase of the feedback mechanism and thus predicts the frequency:

$$f_k = 0.925\sqrt{\frac{\delta}{h}}(k + C_k)^{\frac{3}{2}}\frac{u}{h} \quad (2)$$

where the coefficients for C_k are 0.4, 0.35 and 0.5 for modes $k = 1$, 2 and 3 respectively. Equation 2 does not cover mode 4.

A linear analytical model for predicting the frequency of the edge tone was given by Crichton in [15]. Equation 3 was defined to predict the frequency for modes $k = 1$, 2, 3 and 4. This gives much larger values than Eqn. 2.

$$f_k = \frac{\delta/2}{h}4\pi(k - 0.375)^{\frac{3}{2}}\frac{u}{\delta\pi} \quad (3)$$

Similarly, Howe [16] carried out a linear analysis of the edge tone interactions where the boundaries between the jet and surrounding air were presented as vortex sheets. Equation 4 was derived in [16] to calculate the frequency.

$$f_k \approx 0.92\left(\frac{\delta}{h}\right)^{0.5}(k + 0.54)^{\frac{3}{2}}\frac{u}{h} \quad (4)$$

Vaik et. al. [12, 17] studied the edge tone frequency's dependence on the Reynolds number with respect to the exit width δ, Re_δ and the ratio of h/δ. The Reynolds number is a dimensionless measure of the ratio between the inertia and viscous force in the flow given by:

$$Re_L = \frac{\rho_{air}Lu}{\mu_{air}} \quad (5)$$

where ρ_{air} and μ_{air} are the mass density and dynamic viscosity of air respectively and L is the characteristic dimension of interest, either δ or h in this study. Results from 3D simulations and experiments in [12] confirmed that the flow in the edge tone is 2 dimensional and hence the breadth of the nozzle was not considered.

The equation defined by Vaik et al. [17] to predict the edge tone frequency is given in Eqn. 6.

$$f_k = \left(C_1 - \frac{C_2}{Re_\delta}\right)\left(\frac{1}{h/\delta} - C_3\right)\frac{u}{\delta} \quad (6)$$

The values of the coefficients C_1, C_2 and C_3 are given in [17]. It was found that mode 1 can occur at the same

time as modes 2 and 3 although at a slightly lower frequency, corroborating findings of Brown [13].

No details with regards to the specific bandwidths of the edge tone have been forthcoming from the literature. It is known that for laminar flows the tone will be near a pure tone, conversely for more turbulent flows there will be more small-scale vortices and a wider bandwidth.

2.2 Acoustic Intensity

In [18] Powell defines the following equation for far field sound pressure P in relation to edge tones:

$$|P_k| \simeq \frac{\alpha}{2}\left(\frac{\rho_{air}S_{tk}u^3}{rc}\right)\cos\theta \qquad (7)$$

where the value of $\alpha = 4$ fitted with observed data. The variable c is the speed of sound in air, r is the distance between source and observer, θ is the elevation angle and S_{tk} is the Strouhal number relating to the mode frequency f_k given by:

$$S_{tk} = \frac{f_k\delta}{u} \qquad (8)$$

The relationship between the sound pressure and acoustic intensity was given in [19] as:

$$I = \frac{P^2}{\rho_{air}c} \qquad (9)$$

The acoustic intensity is therefore given by:

$$I_k \simeq \frac{4\rho_{air}S_{tk}^2u^6(\cos\theta)^2}{r^2c^3} \qquad (10)$$

which gives the expected dipole propagation pattern.

3 Impementation

Our model was realised in Pure Data, a real-time graphical data flow programming language ideal for real-time DSP implementation. This was chosen due to the open source nature of the code and ease of repeatability rather than high performance computations. A copy of our edge tone compact sound source can be downloaded at https://code.soundsoftware.ac.uk/projects/edgetone.

The values of h, δ, u, r and θ can all be varied in real-time. They were sampled at 44.1KHz giving $h[n]$, $\delta[n]$, $u[n]$, $r[n]$, $\theta[n]$ where n is the discrete time variable.

Table 1: Comparison of equations for predicting edge tone frequency.

Equation	Absolute error (%)
Brown [13]	11.51
Holger [14]	47.23
Crichton [15]	255.31
Howe [16]	58.85
Vaik et al. [17]	22.56
Best fit; Eqn 12	8.88

3.1 Frequency Calculations

As seen in Section 2.1, there are a number of equations for predicting the frequencies of the different modes. In order to decide which equation to use, we obtained a number of frequency results published in [13, 20–22].

These results had a mixture of wind tunnel measurements and Computational Fluid Dynamics (CFD) simulations, and either a parabolic jet profile or no profile was given. In total 851 results were obtained, in which each data point included airspeed, nozzle exit width and nozzle exit-to-wedge distance.

Table 1 shows the absolute error (%) for all equations mentioned;

$$\text{Absolute error} = \frac{|(f_{\text{predicted}} - f_{\text{published}})|}{f_{\text{published}}} \cdot 100 \quad (11)$$

Brown [13] giving the best results. Using the data obtained from [13, 20–22] we were able to devise an equation to predict S_{tk}. Equation 12 is based on the equation of a best fit surface ($z = C_1 + C_2x + C_3y + C_4x^2 + C_5xy + C_6y^2$), using the same parameters as Vaik et al. [17], Re_δ and h/δ, (Eqn 12).

$$S_{tk} = C_1 + C_2Re_\delta + C_3\left(\frac{h}{\delta}\right) + C_4Re_\delta^2$$

$$+ C_5Re_\delta\left(\frac{h}{\delta}\right) + C_6\left(\frac{h}{\delta}\right)^2 \qquad (12)$$

The values for the coefficients for Eqn 12 for each mode is given in Table 2. The coefficient values were calculated from 200000 iterations using random weight vectors to generate the best fit surface within the 3-dimensional space. The absolute error for this equation was found to be 8.88% which is lower than all other published equations. We used Eqn. 12 in our implementation for predicted modes with parabolic jet profiles.

Table 2: Coefficient values for Eqn. 12

Mode	C_1	C_2	C_3	C_4	C_5	C_6
1	119.38 x10^{-3}	32.14 x10^{-6}	-12.88 x10^{-3}	6.09 x10^{-9}	-3.83 x10^{-6}	436.76 x10^{-6}
2	180.98 x10^{-3}	103.82 x10^{-6}	-11.10 x10^{-3}	-9.41 x10^{-9}	-8.54 x10^{-6}	199.89 x10^{-6}
3	187.38 x10^{-3}	129.94 x10^{-6}	-7.08 x10^{-3}	-13.29 x10^{-9}	-7.47 x10^{-6}	86.48 x10^{-6}
4	187.62 x10^{-3}	181.78 x10^{-6}	-5.09 x10^{-3}	-21.33 x10^{-9}	-8.20 x10^{-6}	47.24 x10^{-6}
5	1.00	-129.43 x10^{-6}	-76.38 x10^{-3}	6.84 x10^{-9}	7.58 x10^{-6}	1.63 x10^{-3}

Since no data was given with top hat profiles, we used Eqn. 6 given in Vaik et al. [17] for this.

Critical to implementing an edge tone model was being able to predict the current mode, mode changes and hysteresis effects. No formula was forthcoming in the literature to predict these properties but a large number of data were available from the results we accumulated to evaluate the frequency prediction equations. Included in this number, Powell [20] also published plots with data points illustrating the mode hysteresis for changes in u and h as measured from wind tunnel experiments.

In [7] it was found that the peak mode of the cavity tone depends on the thickness of the shear layer and airspeed. Since the edge tone is generated by a similar fluid dynamic process, we decided to calculate similar values for the data points gathered; the distance between shear layers Υ and the Reynolds number Re_h. The shear layer is the area of the flow where there is significant gradient of the velocity in the direction of the y-axis. This varies as the air travels from nozzle exit to the wedge, h. For laminar flow the shear layer thickness ξ was given in [23] as $\xi = h^{2/3}$ and for turbulent flows as $\xi = 0.115h$. We calculate $\Upsilon = 2\xi + \delta$.
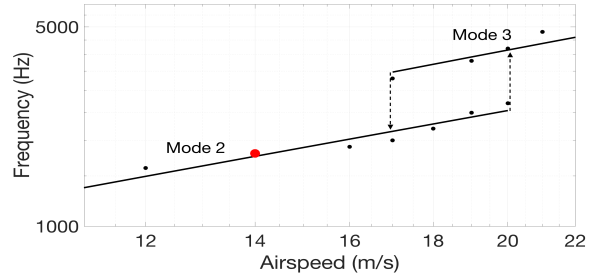
Analysing the 851 data points it was possible to identify modes for each and assign them labels relating to the physical conditions in which they were generated. Data from Powell [20], allowed us to identify conditions where the airspeed was varied or when the distance between the nozzle exit-to-wedge was varied.

In Fig. 4, the larger point shown in red illustrates what can be achieved from a number of circumstances. The red point (around 14 m/s) was obtained when the airspeed was increased through 14 m/s as well as the airspeed decreasing through 14 m/s. It is also reasonable to believe that if the airspeed was steady around 14 m/s that this point would still be achieved.

This labelling technique gives three individual airspeed direction labels for the red point in Fig 4 as shown

Table 3: Example labels for red point given in Figure 4

Reynolds Number Re_h	Jet Thickness Υ	Distance Direction	Airspeed Direction	Mode
7106.35	0.004546893	Static	Up	2
7106.35	0.004546893	Static	Down	2
7106.35	0.004546893	Static	Static	2

Fig. 4: Example of ideal mode changes, including hysteresis, as airspeed u varies with fixed h

in Table 3. Using this labelling scheme, the number of data points increases to 1589. Each data point had five labels; Reynolds Number Re_h, jet thickness at the wedge Υ, u direction, h direction, and an identifying mode number.

All data points were loaded into the Weka machine learning workbench [24] and a decision tree generated to identify mode of operation. The decision tree was implemented based on the result from the Weka classification process. The tree was evaluated using 10 cross fold validation and was found to correctly predict the mode in 82.69% tests with a confusion matrix as shown in Table 4. This gave us a suitable method for predicting the correct mode of operation for the edge tone based on current and changing conditions.

Vaik et al. [25] published conditions on which mode 1 will occur in conjunction with other modes. The Weka workbench [24] created a decision tree to predict if mode 1 should be activated, outputting mode 1 = true if it should be selected. 10-fold cross validation

Table 4: Confusion matrix of the decision tree implemented to select current mode

		Classified as				
		1	**2**	**3**	**4**	**5**
	1	531	60	2	1	0
	2	64	400	49	1	0
Mode	**3**	0	45	287	20	0
	4	1	0	24	61	4
	5	0	0	1	3	35

was carried out and gave 94.49% accuracy. Vaik et al. [17] published coefficient values for calculating the co-existing Mode 1 frequency which were used in the implementation.

3.2 Tone Bandwidth

As stated in Section 2.1, no details of the bandwidth of the tone was forthcoming. Previous research has predicted the tone bandwidth based on measurements for the cavity tone [7]. In the cavity tone air travels over a cavity with air moving at a different velocity within the cavity. The edge tone is a similar fluid dynamic process but air travels as a jet towards a wedge with air at a different velocity on both sides of the jet. The equation used to predict the bandwidth for the cavity tone is:

$$Q_h = 87.715 - 5.296\log(Re_h) \qquad (13)$$

where Q is the value of peak frequency divided by the bandwidth at -3dB, commonly used for signal processing filter design.

But in the edge tone the Reynolds number with respect to the width of the nozzle exit Re_δ is also relevant. From [26] the transition from laminar to turbulent flow was given at a value of $Re_h = 25000$. Applying this to Eqn. 13 gives value of $Q_h \approx 34$.

It was stated in [27] that a flow with $Re_\delta = 3000$ is laminar. The highest value in the data gathered from Powell [20] is $R_{e\delta} = 4000$ and a value of $Re_\delta = 6000$ was labelled turbulent in [28]. We therefore estimated a critical value for Re_δ of 5000 and assigned Q_δ the same critical value as for Q_h. A fully laminar flow of $Re_\delta = 50$ was assigned a $Q_\delta = 90$ which allowed us to derive an equation to estimate the Q with respect to Re_δ, labelled Q_δ.

$$Q_\delta = 137.571 - 12.1602\log(Re_\delta) \qquad (14)$$

An average value from both Eqns. 13 and 14 was calculated to obtain the final Q value, $Q = (Q_h + Q_\delta)/2$.

3.3 Acoustic Intensity

Equation 10 in Section 2.2 was implemented in a discrete form to calculate the acoustic intensity of the edge tone dipole source.

3.4 Final Output

To implement the final synthesis model a single noise source $W[z]$ was used for the sound source. The decision tree selects the mode and the correct coefficient values are chosen for Eqn. 12 from Table 2 for the parabolic profile. Equation 6 was used for the top hat profile and when mode 1 tones co-exist with other modes as illustrated by ‡.

The predicted frequency was designated as the centre frequency for a bandpass filter $B_k[z]$ which was applied to the noise source. The output from this is given by:

$$X_k[z] = W[z]B_k[z] \qquad (15)$$

where the discrete time output $x_k[n]$ is given by the inverse z-transform on $X_k[z]$. The Q value of the bandpass filter was calculated in Section 3.2. The final output is given by:

$$y[n] = \begin{cases} \Lambda(x_1[n]^{\ddagger} + x_k[n]), & \text{co-existing modes = true} \\ \Lambda\, x_k[n], & \text{otherwise} \end{cases}$$
$$(16)$$

where Λ is a user defined variable allowing the gain to be adjusted for artistic purposes. $x_1[n]^{\ddagger}$ was set from Eqn. 6 which was the only study giving a measured prediction for co-existing modes.

As stated in Section 2.1, Brown [13], the ratio range of h/δ was found to be 3.5–60. The 851 results obtained from [13, 20–22] were examined and the range of h/δ was found to be from 2–60.6 therefore limits on the model were set to $\approx$ 2–61.

4 Results

Figures 5 and 6 compare published results from Powell [20] with those from our model under circumstances where the airspeed u was increased and decreased. Since the scenarios in which mode 1 co-exists with modes 2 and 3 were not included in the originals they were omitted from results of our models to enable a clearer comparison.

The decision tree for selecting the correct modes under the changing airspeed appears to give excellent results. Note that the points for the published data from [20]
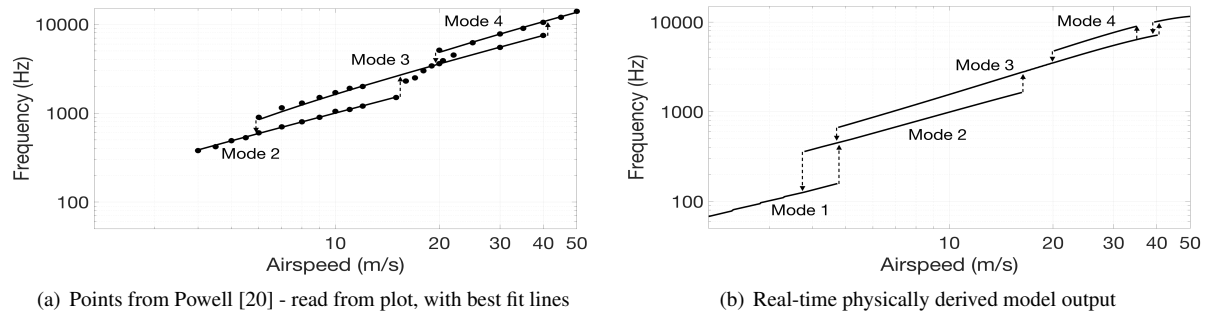
(a) Points from Powell [20] - read from plot, with best fit lines
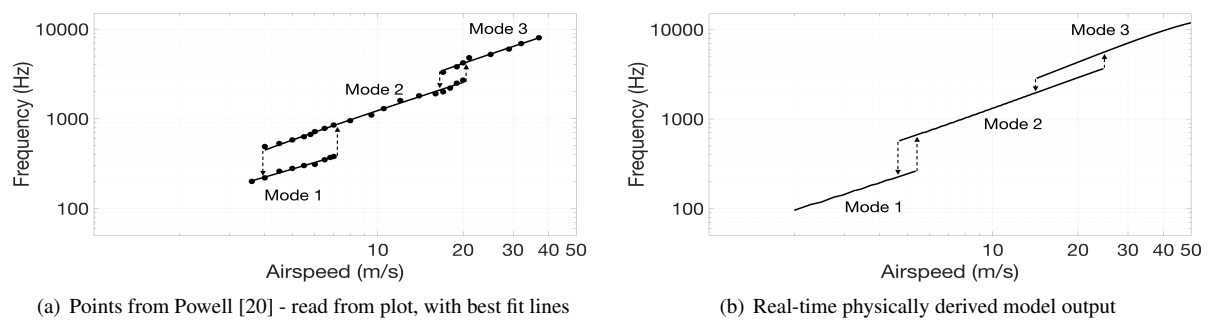

(b) Real-time physically derived model output

Fig. 5: Mode changes, including hysteresis, in edge tone when varying airspeed u. Nozzle exit width, $\delta =$ 0.00104m; Nozzle exit to wedge distance, $h = 0.01$m.

(a) Points from Powell [20] - read from plot, with best fit lines

(b) Real-time physically derived model output

Fig. 6: Mode changes, including hysteresis, in edge tone when varying airspeed u. Nozzle exit width, $\delta =$ 0.00099m; Nozzle exit to wedge distance, $h = 0.0075$m.

have been read from a plot and this will have added some minor noise.

From Figs. 5(a) and 5(b) we see that the mode changes from 2 to 3 then to 4 and back down again. All occur at virtually the same airspeed and frequency to that given by Powell [20]. An anomaly was seen when decreasing the airspeed while in mode 4. Here the mode momentarily drops down to mode 3 before rising back up to mode 4 and continuing at expected frequency values. This highlights an area where the decision tree predicting the mode has produced an error. When in mode 2 and the airspeed was decreased below 4 m/s, our model drops to mode 1 which is a highly plausible example of our model working beyond the training data.

Similar results can be seen from Figs. 6(a) and 6(b) where our model gives excellent results. The main difference was the size of the hysteresis loop was smaller between modes 1 and 2, and larger between mode 2 and 3.

In Figs. 7 and 8 the nozzle exit-to-wedge distance h was increased and decreased showing the changes in modes

and frequencies. Although results from our model are similar the hysteresis loops were larger between modes except modes 4 and 5. A discrepancy was seen while increasing h in mode 2 where the mode briefly changed to mode 3 and back in the middle of the hysteresis loop. The distances for mode changes were similar to experimental values as were the predicted tone frequencies.

Figures 8(a) and 8(b) show a larger divergence between experimental results and our model. The changes from modes 1 through to 4 are at relatively similar values with respect to h but the equation for the predicted frequencies is less accurate. It is believed this is due to flaws in the Re_h and h/δ best fit surface used to predict the tone frequency under these operating conditions.

A comparison of the Sound Pressure Level (SPL) between our model and measured values given in [20] is illustrated in Fig. 9. The main difference in our implementation was that the SPL increased faster than witnessed by Powell [20]. The mode changes occur at approximately the same airspeed u and it can be seen that our model changed to mode 4 as the airspeed past 54 m/s.
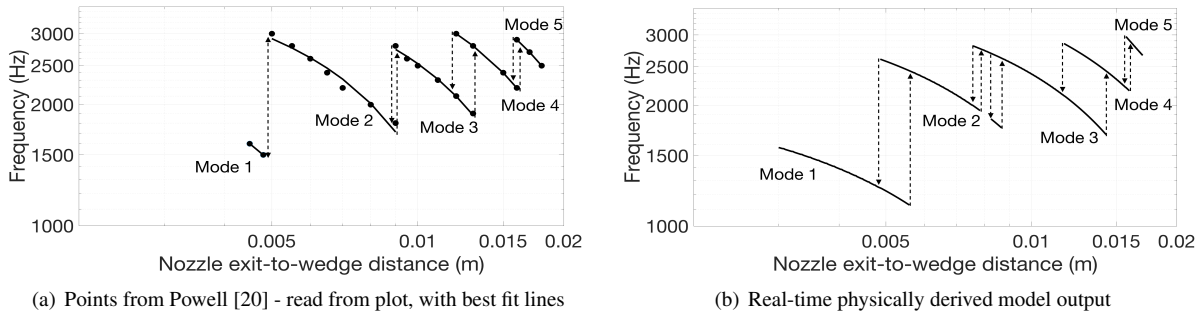
(a) Points from Powell [20] - read from plot, with best fit lines

(b) Real-time physically derived model output

Fig. 7: Mode changes, including hysteresis, in edge tone when varying nozzle exit to wedge distance h. Nozzle exit width, $\delta = 0.00106$m; Airspeed, $u = 14.48$m/s.

(a) Points from Powell [20] - read from plot, with best fit lines
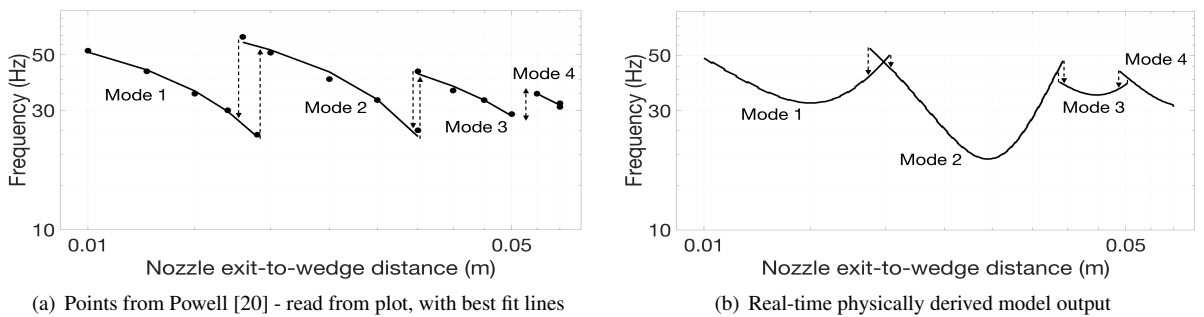

(b) Real-time physically derived model output

Fig. 8: Mode changes, including hysteresis, in edge tone when varying nozzle exit to wedge distance h. Nozzle exit width, $\delta = 0.00099$m; Airspeed, $u = 1.45$m/s.
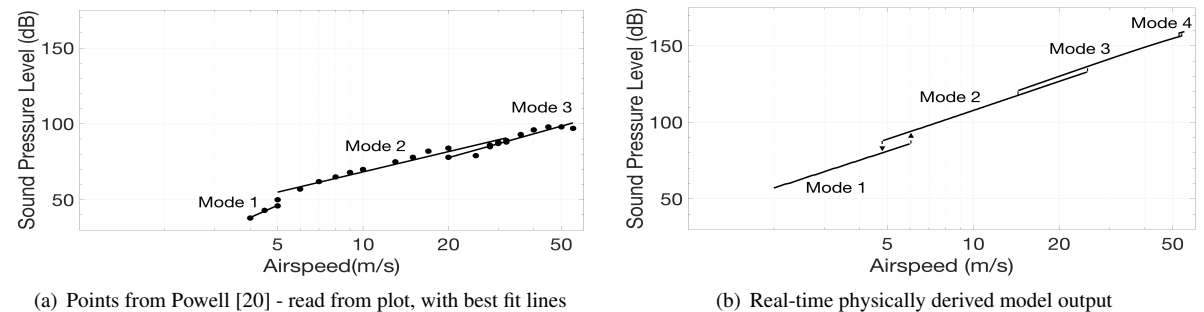

(a) Points from Powell [20] - read from plot, with best fit lines

(b) Real-time physically derived model output

Fig. 9: Sound pressure level with increasing airspeed u. Nozzle height $\delta = 0.000104$m; nozzle to wedge distance h = 0.0075m; distance r = 0.2m; elevation $\theta = 0°$; user gain $\Lambda = 1$.

5 Discussion

Analysis of the results presented in Section 4 shows that compared to experimental results published in [20] our physically derived model performs very well. The greatest errors appear to occur when operating at very slow airspeed. Results presented in Fig. 8 were produced with $u = 1.45$ m/s compared to an average of 12.76 m/s for the data used to create Eqn. 12. In Fig. 5(a) the lowest experimental airspeed was 4 m/s and our model was able to predict this accurately and

indeed decrease down to 2 m/s and still appear accurate.

The mode changes modelled in Figs. 5 to 8 indicate that our model is accurate in predicting the current mode of operation. We are also able to model the hysteresis when changing modes from either increasing or decreasing u or increasing or decreasing h. This is the first edge tone synthesis model we are aware of that predicts the mode of operation and is able to portray hysteresis.

The differences in the frequency equations outlined in Section 2.1 highlight the difficulty in predicting the tone frequency. The jet profile is also known to make a difference to the observed frequency. The equation presented in [17] was the only one of those examined that had separate coefficients for the top hat profile and parabolic profile.

Our best fit equation was derived for experimental and simulated results which were either had parabolic or unknown jet profiles. Equations defined by Brown [13], Holger [14] and Vaik et al. [17] are limited to predicting frequencies in modes 4, 3 and 4 respectively. Our equation is able to predict up to and including mode 5. Under certain circumstances, Eqn. 12 was found to produce negative frequencies. This is due to the nature of the errors within the best fit surface used to define it. A low threshold of 0 Hz was set during implementations to prevent this occurring.

Using Eqn. 12 for the parabolic jet profile gives the most accurate frequency prediction for the majority of operating conditions including predictions for unknown jet profiles. Using Eqn. 6 for the top hat profile as well as circumstances when mode 1 co-exists with other modes gives the most accurate replication for the widest range of operating scenarios.

The higher SPL values witnessed from our model in Fig. 9 can be attributed to the constant value of α assigned by Powell [18] to 4. It is also noted that Powell [18] gives Eqn. 7 as approximately equal to the pressure and there may be additional variables between measured and theoretical values.

Ideal evaluation of our model would include a wide variety of wind tunnel tests with a number of edge tone geometries; varying airspeeds and distances between nozzle and wedge. Included in any tests should be measurements of the tone bandwidth in order that a more accurate synthesis of this property could be developed. It would be worthwhile to evaluate results from the synthesis model to conditions far from the ones examined, with higher airspeeds, past the critical Reynolds numbers to more turbulent regimes. This would also enable us to gather more data and improve the model equation for frequency prediction and mode selection.

Coupling the edge tone to a synthesis model of a resonator, exciting modes and replicating flue instruments would be an area for future development. This could be extended to a synthesis model of a pipe organ similar to [29], examining our edge tone model as an excitation compared to the white noise source used in [29]. This could have particular perceptual consequences to note transients compared to previous physical models.

6 Conclusion

A physically derived synthesis model of an edge tone was presented. A number of frequency prediction equations were tested and a best fit equation was proposed giving a lower absolute error than those previously published. Machine learning techniques were utilised to predict the mode changes due to changes in the geometry of the edge tone and the fluid dynamics feedback system.

Excellent results have been found when compared to measured data published by an extensive study by Powell [20]. Errors have been identified from our test results along with areas for future development.

References

[1] Selfridge, R., Moffat, D., and Reiss, J. D., "Real-time Physical Model for Synthesis of Sword Swing Sounds," in *14th Sound and Music Computing*, pp. 1–7, 2017.

[2] Selfridge, R., Moffat, D., and Reiss, J. D., "Physically Derived Sound Synthesis Model of a Propeller," in *Proceedings of the 12th International Audio Mostly Conference on Augmented and Participatory Sound and Music Experiences, 23-26 August, London, UK*, 16, pp. 16:1–16:8, ACM, 2017.

[3] Selfridge, R. et al., "Real-Time Physical Model of an Aeolian Harp," *24th International Congress on Sound and Vibration, London*, pp. 1–8, 2017.

[4] Curle, N., "The influence of solid boundaries upon aerodynamic sound," *Proceedings of the Royal Society of London A: Mathematical, Physical and Engineering Sciences*, 231(1187), 1955.

[5] Crighton, D. et al., *Modern methods in analytical acoustics: lecture notes*, Springer Science &; Business Media, 2012.

[6] Selfridge, R. et al., "Physically Derived Synthesis Model of an Aeolian Tone." in *Audio Engineering Society Convention 141*, pp. 1–10, 2016.

[7] Selfridge, R., Reiss, J., and Avital, E., "Physically Derived Synthesis Model of a Cavity Tone," in *Proceedings of the 20th Digital Audio Effects Conference, Edinburgh, UK*, pp. 5–9, 2017.

[8] Selfridge, R., Moffat, D., and Reiss, J. D., "Sound Synthesis of Objects Swinging through Air Using Physical Models," *Applied Sciences*, 7(11), p. 1177, 2017.

[9] Ystad, S., "Sound modeling applied to flute sounds," *Journal of the Audio Engineering Society*, 48(9), pp. 810–825, 2000.

[10] De La Cuadra, P. et al., "A physical model and experimental testbed for real-time simulation of flute-like instruments," *The Journal of the Acoustical Society of America*, 117(4), p. 2414, 2005.

[11] Ibrahim, M. K., "Experimental and Theoretical Investigations of Edge Tones in High Speed Jets," *Journal of Fluid Science and Technology*, 8(1), pp. 1–19, 2013.

[12] Vaik, I., Varga, R., and Paál, G., "Frequency and Phase Characteristics of the Edge Tone, Part I," *Periodica Polytechnica. Engineering. Mechanical Engineering*, 58(1), p. 55, 2014.

[13] Brown, G. B., "The vortex motion causing edge tones," *Proceedings of the Physical Society*, 49(5), 1937.

[14] Holger, D. K., Wilson, T. A., and Beavers, G. S., "Fluid mechanics of the edgetone," *The Journal of the Acoustical Society of America*, 62(5), pp. 1116–1128, 1977.

[15] Crighton, D., "The jet edge-tone feedback cycle; linear theory for the operating stages," *Journal of Fluid Mechanics*, 234, pp. 361–391, 1992.

[16] Howe, M., "Edge, cavity and aperture tones at very low Mach numbers," *Journal of Fluid Mechanics*, 330, pp. 61–84, 1997.

[17] Vaik, I., Varga, R., and Paál, G., "Frequency and Phase Characteristics of the Edge Tone, Part II," *Periodica Polytechnica. Engineering. Mechanical Engineering*, 58(1), p. 69, 2014.

[18] Powell, A., "On the edgetone," *The Journal of the Acoustical Society of America*, 33(4), pp. 395–409, 1961.

[19] Goldstein, M., "Aeroacoustics," *New York, McGraw-Hill International Book Co.,*, 1976.

[20] Powell, A. et al., "An experimental study of low speed edgetones," Technical report, California University Los Angeles, 1964.

[21] Dougherty, N., Liu, B., and Ofarrell, J., "Numerical simulation of the edge tone phenomenon," Technical report, NASA Contractor Report 4581, 1994.

[22] Bamberger, A., Bänsch, E., and Siebert, K., "Experimental and numerical investigation of edge tones," *Journal of Applied Mathematics and Mechanics*, 84(9), pp. 632–646, 2004.

[23] Cebeci, T. and Bradshaw, P., *Physical and computational aspects of convective heat transfer*, Springer Science & Business Media, 2012.

[24] Holmes, G., Donkin, A., and Witten, I. H., "Weka: A machine learning workbench," in *Intelligent Information Systems, 1994. Proceedings of the 1994 Second Australian and New Zealand Conference on*, pp. 357–361, IEEE, 1994.

[25] Vaik, I. and Paál, G., "Mode switching and hysteresis in the edge tone," *Journal of Physics: Conference Series*, 268(1), p. 012031, 2011.

[26] Schlichting, H. et al., *Boundary-layer theory*, Springer, 1960.

[27] Suponitsky, V., Avital, E., and Gaster, M., "Hydrodynamics and sound generation of low speed planar jet," *Journal of Fluids Engineering*, 130(3), p. 031401, 2008.

[28] Thomas, F. and Goldschmidt, V., "Structural characterisics of a developing turbulent planar jet," *Journal of Fluid Mechanics*, 163, pp. 227–256, 1986.

[29] Valimaki, V. et al., "A real-time DSP implementation of a flute model," in *IEEE International Conference on Acoustics, Speech, and Signal Processing*, volume 2, pp. 249–252, 1992.